

## De Novo Design and Spectroscopic Characterization of a Dinucleating Copper-Binding Pentadecapeptide

David A. Rockcliffe,\*† Arthur Cammers,‡ Ayaluru Murali,† William K. Russell,† and Victoria J. DeRose†

Department of Chemistry, Texas A&amp;M University, College Station, Texas 77842-3012, and Department of Chemistry, University of Kentucky, Lexington, Kentucky 40506

Received September 14, 2005

A spectroscopic study of aqueous solutions of Ac–WGHGHGH–GPGHGHGH–NH<sub>2</sub> (HGP) indicates that copper(II) binds to the peptide to form a 2:1 Cu<sup>2+</sup>/HGP complex with four nitrogen atoms in the copper coordination environment. Electron paramagnetic resonance (EPR) and UV–visible data suggest copper binding through the peptide backbone and imidazole nitrogen donors. Circular dichroism data show that HGP is unbound below pH 5.5 and is copper-saturated at pH 9 and above. The apo form of the peptide is unstructured in solution and is organized into a turn conformation in the presence of 2 mol equiv of Cu<sup>2+</sup> at basic pH. EPR measurements for 2:1 Cu<sup>2+</sup>/HGP solutions in the *g* = 2 region and within the pH range 7–11 exhibit axial spectra. A molecular-mechanics-minimized model of the Cu<sup>2+</sup>/HGP complex gave a Cu···Cu separation of 8 Å.

Several classes of histidine-bound copper-containing proteins and enzymes are involved in the processing of dioxygen including dioxygen transport, monooxygenation, dioxygenation, and oxidation.<sup>1</sup> X-ray analyses of the active site of hemocyanins (the oxygen carrier in mollusks and arthropods) show a side-on Cu<sub>2</sub>–μ–η<sup>2</sup>:η<sup>2</sup>–O<sub>2</sub> copper binding motif in which each copper ion is coordinated to the imidazole group of three histidine residues.<sup>2</sup> Tyrosinase, which catalyzes the hydroxylation of phenols and the oxidation of catechols, is considered to have an analogous active site structure. General interest in investigating the functioning of oxygen processing proteins and enzymes is due to their important roles in biochemistry<sup>1,3,4</sup> and potential application to industrial and organic synthesis.<sup>5,6</sup> Synthetic models for the active site of hemocyanin have been prepared mostly with imine- and

pyridine-type nitrogen donors.<sup>7</sup> Our interest is in the preparation and investigation of more biotic model complexes for oxyhemocyanin in an attempt to discover the minimal peptide binding motif that spectroscopically and functionally represents the protein active site. Important to the study is the strategic placement of histidine on the designed peptide and its ability to form a dinuclear binding site that results in a close Cu···Cu separation.

The peptide HGP was designed with the sequence WGH–GHGHGPGHGHGH and was prepared as the C-terminal amide and acetylated at the N terminus. This peptide design encompasses two binding domains for Cu<sup>2+</sup>, each containing three coordinating histidine residues. The peptide as a whole, has a proline residue designed to form the center of a β-turn conformation that presents two copper ions in relatively close proximity. Glycine was chosen as the intervening residue between histidines because it is less sterically hindered than other amino acids and gives the peptide greater conformational freedom. The N-terminus tryptophan was used as a tag for peptide concentration determinations.

The nature of aqueous solution peptide species is known to be strongly pH-dependent.<sup>8</sup> The UV–circular dichroism (CD) spectrum of aqueous solutions of HGP in the absence of Cu<sup>2+</sup> shows a positive band of moderate intensity with a maximum of around 222 nm (Figure 1). The features of the CD spectrum are indicative of a random-coil structure and do not change appreciably with changes in the pH. By contrast, solutions of HGP in the presence of 2 mol equiv of Cu<sup>2+</sup> display turn conformation features<sup>9</sup> of a positive ellipticity at 209 nm and a less intense negative band around 228 nm when recorded between pH 7 and 8. A shift is observed in the negative ellipticity to 224 nm for pH 9. X-band electron paramagnetic resonance (EPR) spectra of HGP in the presence of 2 mol equiv of Cu<sup>2+</sup> (Figure S1 in

\* To whom correspondence should be addressed. E-mail: david.rockcliffe@kysu.edu. Current address: Division of Mathematics and Sciences, Kentucky State University, Frankfort, KY 40601.

† Texas A&M University.

‡ University of Kentucky.

- (1) Solomon, E. I.; Sundaram, U. M.; Machonkin, T. E. *Chem. Rev.* **1996**, *96*, 2563–2605.
- (2) Magnus, K.; Hazes, B.; Ton-That, H.; Bonaventura, C.; Bonaventura, J.; Hol, W. G. J. *Proteins* **1994**, *19*, 302–309.
- (3) Klinman, J. P. *Chem. Rev.* **1996**, *96*, 2541–2561.
- (4) Solomon, E. I.; Chen, P.; Metz, M.; Lee, S.-K.; Palmer, A. E. *Angew. Chem., Int. Ed.* **2001**, *40*, 4570–4590.

(5) *Bioinorganic Chemistry of Copper*; Karlin, K. D., Tyeklar, Z., Eds.; Chapman & Hall: New York, 1993.

(6) Kitajima, N.; Moro-Oka, Y. *Chem. Rev.* **1994**, *94*, 737–757.

(7) Mirica, L. M.; Ottenwaelder, X.; Stack, T. D. *Chem. Rev.* **2004**, *104*, 1013–1045.

(8) Kozłowski, H.; Bal, W.; Dyba, M.; Kowalik-Jankowska, T. *Coord. Chem. Rev.* **1999**, *184*, 319–346.

(9) Dyson, H. J.; Wright, P. E. *Annu. Rev. Biophys. Biophys. Chem.* **1991**, *20*, 519–538.

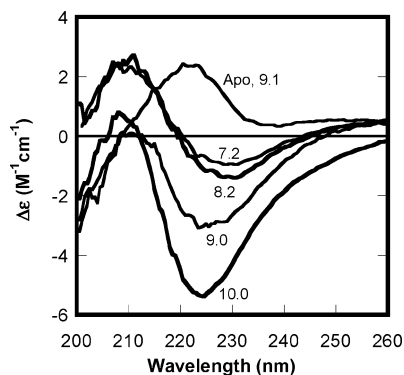


**Figure 1.** CD spectra of 2:1  $\text{Cu}^{2+}$ /HGP solutions of Cu-HGP (20  $\mu\text{M}$ ) within the pH range 7–10 compared with the apo-peptide at pH 9.1. The pH values are indicated on the curves.

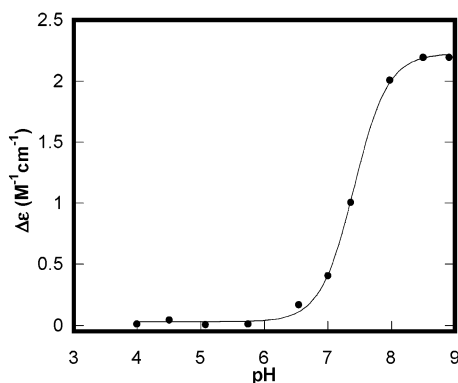


**Figure 2.** Cu/HGP pH dependence of  $\Delta\epsilon$  at 344 nm. The pH dependence data were fit to the equation  $\Delta\epsilon = \{\Delta\epsilon_{\text{acid}}[\text{H}^+]^n + \Delta\epsilon_{\text{base}}K_a^n\}/\{[\text{H}^+]^n + K_a^n\}$ , where  $n$  is the Hill coefficient and  $K_a$  is the acid dissociation constant. The midpoint of the transition is 7.4.

the Supporting Information) show that below pH 6 the solution contains a mixture of aqueous and complexed  $\text{Cu}^{2+}$ . Above pH 6, there is copper coordination to the peptide, forming a species that persists until approximately pH 10, where the value of  $g_{\text{II}}$  decreases and a new species emerges. An identical trend is observed for the electronic absorption spectra recorded between pH 4 and 11 (Figure S2 in the Supporting Information). At low pH values, the solution spectrum is characterized by a broad weak band that indicates aqueous  $\text{Cu}^{2+}$  as the dominant species. As the pH is increased, a shorter-wavelength band grows in and the maximum absorption shifts to 564 nm at pH values between 8 and 9. Above pH 9, there is a further shift in the absorption maximum to 556 nm, indicating a change in the coordination environment for  $\text{Cu}^{2+}$ . In general, CD, EPR, and electronic absorption spectra demonstrate that the binding of copper is strongly pH-dependent.

Visible CD spectroscopy was used to examine the Cu/HGP speciation between pH values of 6 and 10. Figure 2 shows the result of a pH titration of 2:1  $\text{Cu}^{2+}$ /HGP solutions followed by visible CD spectroscopy at  $\lambda_{\text{max}} = 344$  nm. The data can be fit to a model of pH-dependent  $\text{Cu}^{2+}$  binding to HGP, which shows a deprotonation event with  $\text{p}K_a = 7.4$ . The Hill coefficient of 1.6 suggests a moderate cooperativity, with respect to  $\text{H}^+$ , for the transition between the unbound species below pH 6 and the fully bound copper complex at pH 8.5 and above. Above pH 9.5, there is a shift in the 344-

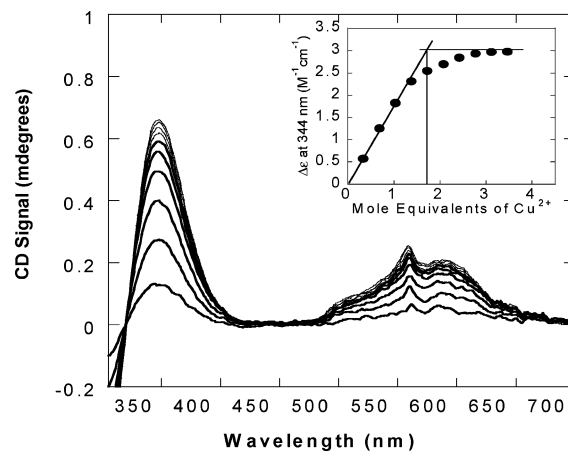


**Figure 3.**  $\text{Cu}^{2+}$  addition to a solution of HGP (200  $\mu\text{M}$ ) at pH 9.2 followed by CD. Inset: Binding curve showing the dependence of  $\Delta\epsilon$  at 344 nm on the mole equivalents of added  $\text{Cu}^{2+}$ . The  $\text{Cu}^{2+}$  saturation point is at 1.8 mol equiv.

nm band of the visible CD spectrum, and an isosbestic point develops at 335 nm, which represents a transition to a new species (data not shown).

Several lines of evidence indicate that HGP binds two  $\text{Cu}^{2+}$  ions at pH values above 7. Copper(II) titrations of a solution of HGP at pH 9.2 were followed by visible CD. The results show that the positive ellipticity at 344 nm increases to a maximum of  $3.1 \text{ M}^{-1} \text{ cm}^{-1}$  (Figure 3). An analysis of the binding curve at  $\lambda_{\text{max}} = 344$  nm gives the copper saturation point as 1.8 mol equiv of  $\text{Cu}^{2+}$  (Figure 3).

Related studies were conducted with EPR spectroscopy where spectra were obtained as a function of  $\text{Cu}^{2+}$  titrated into a solution of HGP at pH 10.1. The results show that, upon an increase in the amount of added  $\text{Cu}^{2+}$ , the line shape of the spectrum is invariant as the spectral intensity increases. The integrated intensity increases in an approximately linear manner until the addition of 2 mol equiv of  $\text{Cu}^{2+}$  (Figure S4 in the Supporting Information). An additional investigation of the  $\text{Cu}^{2+}$ /HGP binding stoichiometry was conducted with electronic absorption spectroscopy. Similar to the CD experiments,  $\text{Cu}^{2+}$  titrated into a solution of HGP at pH 9.7 was monitored by UV-visible at 564 nm. The absorbance of the solution increased until approximately 2 mol equiv of  $\text{Cu}^{2+}$  were added (Figure S4 in the Supporting Information). The results of analyses by mass spectrometry show a major peak at  $m/z = 844.7$  that is attributed to  $[\text{Cu}_2/\text{HGP}]^{2+}$  (data not shown). This is observed as the dominant species within the pH range 7–10. On the basis of saturation data obtained from CD, UV-visible, EPR, and mass spectrometry spectra at 2 equiv of  $\text{Cu}^{2+}$ , it is concluded that HGP is a dinucleating peptide.

The ligand donor set in Cu/HGP, which was designed to bind each Cu ion through three histidine ligands, can also be predicted based on parameters from EPR, CD, and UV-visible spectroscopies. Copper(II) EPR spectra obtained for Cu/HGP are axial, indicating a tetragonal or square-pyramidal environment with either weakly binding or no axial ligands. The UV-visible data illustrate that ligand binding is initiated around pH 6. Analysis by mass spectrometry at pH 6 reveals a dominant peak at  $m/z = 813.7$  amu that is attributed to a

## COMMUNICATION

mononuclear  $[\text{CuL}]^{2+}$  species. Because the  $\text{p}K_{\text{a}}$  for imidazole is  $\sim 7$ , the UV–visible and mass spectrometry results indicate that copper is most likely binding to histidine at this pH value. The anisotropic spin-Hamiltonian parameters (Table S1 in the Supporting Information) exhibit values of  $g_{\parallel}$  and  $A_{\parallel}$  that are very similar for all species present at pH 7.1 and 9.2, indicating little change in the coordination environment over this pH range. In contrast, there is a significant decrease in  $g_{\parallel}$  for the species at pH 11.1. The measured values of  $g_{\parallel}$  and  $A_{\parallel}$  were applied to Peisach–Blumberg correlations<sup>10</sup> in order to establish the donor atoms for copper. This analysis suggests that for the species at pH 7.1, 9.2, and 11.1 a 4N copper environment is the most likely binding arrangement, although a 3N 1O environment cannot be ruled out. Nitrogen binding to copper is possible through the peptide backbone amide groups as well as through the histidine imidazole side-chain group.<sup>11,12</sup> The presence of both types of nitrogen binding in Cu/HGP is suggested by the CD spectrum at pH 9.2, where charge-transfer bands at 300 nm ( $\text{N}_{\text{amide}} \rightarrow \text{Cu}^{2+}$ ) and 344 nm ( $\text{N}_{\text{im}} \rightarrow \text{Cu}^{2+}$ )<sup>13</sup> are observed. Additional evidence of imidazole and backbone nitrogen coordination is provided by the wavelength maximum of the  $\text{Cu}^{2+} \text{d} \rightarrow \text{d}$  transition in the visible absorption spectrum. Studies with short peptides show that  $\lambda_{\text{max}}$  values for the visible absorption spectra range from 540 nm for 4N to 765 nm for 1N complexes that involve nitrogen atoms supplied by the peptide backbone and the imidazole side chain of histidine.<sup>14</sup> At pH 9.3, the Cu/HGP complex displays an absorption maximum at 566 nm, which is red-shifted relative to the 4N complex, Cu/Ac-GGGH, whose absorption maximum occurs at 545 nm. Copper binding in the latter case is considered to be through three backbone nitrogen atoms and a nitrogen atom from imidazole. The stronger ligand field provided by N(backbone) relative to N(imidazole) explains the red-shifted Cu/HGP absorption band at 566 nm, which is interpreted as being associated with an environment containing less than three backbone nitrogen atoms. The different types of nitrogen units engaged in copper binding are also inferred from mass spectrometry, which gave a  $m/z = 844.7$  amu peak dominating at pH values between 7 and 9. This peak corresponds to a  $[\text{Cu}/\text{HGP} - 2\text{H}]^{2+}$  species, where there is most likely deprotonation of two backbone amide nitrogen atoms. In addition, equatorial coordination of  $\text{OH}^-$  or  $\text{H}_2\text{O}$  was not detected by mass spectrometry, although loss of an axial ligand during ionization cannot be ruled out.<sup>15</sup> Taken together, the coordination environment for each copper ion in Cu/HGP is predicted to consist of three imidazole nitrogen atoms and one amide nitrogen atom.

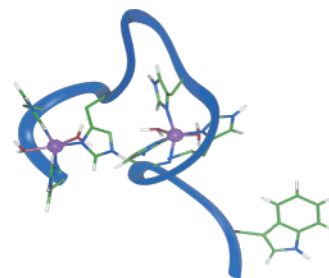


**Figure 4.** Energy-minimized model of the Cu/HGP complex showing the copper binding region and the turn conformation.

The combined information from these measurements was used to construct an energy-minimized structure of the Cu/HGP complex. The propensity for copper to bind to the backbone nitrogen of histidine itself and the backbone nitrogen of residues N terminal to it was taken into account.<sup>16</sup> The proposed structure (Figure 4) shows each  $\text{Cu}^{2+}$  ion binding to three imidazole groups and one backbone amide nitrogen group. The structure also shows a turn, as supported by CD data, that is assumed to incorporate a proline residue. The turn places the  $\text{Cu} \cdots \text{Cu}$  separation at approximately 8 Å. The structure was energy optimized by considering various amide binding positions on the peptide while keeping the donor atom set constant.

In summary, we have designed and investigated the  $\text{Cu}^{2+}$  binding characteristics of a dinculeating peptide, HGP. The peptide is unstructured in solution and binds copper in a 2:1  $\text{Cu}^{2+}/\text{HGP}$  ratio with a concomitant conformational change. Each  $\text{Cu}^{2+}$  is coordinated through three imidazole nitrogens and one backbone nitrogen. Energy minimization studies show that the turn conformation could bring the  $\text{Cu}^{2+}$  ions within 8 Å of each other. To our knowledge, this is the first example of a designed oligopeptide for which a dinucleating capability has been established. This unique system is being developed as a synthetic model for type III copper sites in proteins and enzymes.

**Acknowledgment.** The authors thank Dr. Marty Scholtz and his research group for assistance with CD spectroscopy. This work was supported by the NIH (Grant F33 GM072286-01, which includes a Ruth L. Kirschstein National Research Service Award for D.A.R., and Grant T32 GM008523) and the Robert A. Welch Foundation (V.J.D.). EPR facilities at Texas A&M University are supported by the NSF (Grant CHE-0092010).

**Supporting Information Available:** X-band EPR spectra of HGP in the presence of 2 mol equiv of  $\text{Cu}^{2+}$  (Figure S1), electronic absorption spectra recorded between pH 4 and 11 (Figure S2), titrations of solutions of HGP with  $\text{Cu}^{2+}$  followed by X-band EPR (Figure S3),  $\text{Cu}^{2+}$  titration of a solution of HGP (initially 600  $\mu\text{M}$ ) followed by UV–visible absorption spectroscopy at pH 9.7 (Figure S4),<sup>17</sup> and anisotropic spin-Hamiltonian parameters (Table S1). This material is available free of charge via the Internet at <http://pubs.acs.org>.  
IC051577Q

(16) Bryce, G. F.; Roeske, R. W.; Gurd, R. N. *J. Biol. Chem.* **1965**, *240*, 3837–3846.

(17) Reference for EPR spectral simulations (Figure S4 in the Supporting Information). Stoll, S. *Spectral Simulations in Solid-State EPR*. Ph.D. Thesis, ETH Zurich, Zurich, Switzerland, 2003.

(10) Peisach, J.; Blumberg, W. E. *Arch. Biochem. Biophys.* **1974**, *165*, 691–708.

(11) Burns, C. S.; Aronoff-Spencer, E.; Dunham, C. M.; Lario, P.; Avdievich, N. I.; Antholine, W. E.; Olmstead, M. M.; Vrieling, A.; Gerfen, G. J.; Peisach, J.; Scott, W. G.; Millhauser, G. L. *Biochemistry* **2002**, *41*, 3991–4001.

(12) Sigel, M.; Martin, R. B. *Chem. Rev.* **1982**, *82*, 385–426.

(13) Syme, C. D.; Nadal, R. C.; Rigby, S. E. J.; Viles, J. H. *J. Biol. Chem.* **2004**, *279*, 18169–18177.

(14) Bryce, G. F.; Gurd, F. R. N. *J. Biol. Chem.* **1966**, *241*, 122–129.

(15) Bonomo, R. P.; Cucinotta, V.; Giuffrida, A.; Impellizzeri, G.; Magri, A.; Pappalardo, G.; Rizzarelli, E.; Santoro, A. M.; Tabbi, G.; Vagliasindi, L. *Dalton Trans.* **2005**, 150–158.